Aalborg Universitet

On Polarization and Frequency Dependence of Diffuse Indoor Propagation

Nielsen, Jesper Ødum; Andersen, Jørgen Bach; Pedersen, Gert Frølund; Pelosi, Mauro

On Polarization and Frequency Dependence of Diffuse Indoor Propagation

Jesper Ødum Nielsen, Jørgen Bach Andersen, Gert Frølund Pedersen, Mauro Pelosi
APNet, Department of Electronic Systems
Faculty of Engineering and Science
Aalborg University
DK-9220 Aalborg, Denmark
Email: jni@es.aau.dk

Abstract—The room electromagnetics (RE) theory describes the radio propagation in a single room assuming diffuse scattering. A main characteristic is the exponential power-delay profile (PDP) decaying with the so-called reverberation time (RT) parameter, depending only on the wall area, the volume of the room and an absorption coefficient. The PDP is independent on the location in the room, except for the arrival time. Based on measurements in a room with a spherical array of 16 dual-polarized wideband horn antennas, the current work studies how the RE parameters depend on the receiver (Rx) antenna polarization and orientation. Also the frequency dependence is investigated, with measurements done at both 2.3 GHz and 5.8 GHz center frequencies. The RE theory was found to fit well to the measurements with a RT in the range 22-25 ns. Only small differences were found due to the polarization and the channel gain was depending approximately as expected with frequency.

I. Introduction

The indoor wideband radio propagation channel is crucial to any communications system utilizing the radio channel, such as a wireless local area network (WLAN), and knowledge of the channel may be needed not only for deployment of systems, but for also investigation of the performance of proposed systems and methods.

Knowledge of the channel may be obtained via radio channel measurements, but these may be expensive and difficult to carry out. As an alternative, the so-called ray-tracing methods are often used to predict specular signal components via calculation of free space losses, reflections on walls *etc.*, and diffractions [1]. It has been recognized that predicting the channel in this way often does not produce sufficiently accurate results. In order to improve the results, the concept of diffuse scattering has been introduced, both to include the effects of surface roughness and random minor objects in the environment not included in the general information about building environment [2], [3]. While detailed knowledge of the environment structure and material properties is a prerequisite for ray-tracing, inclusion of diffuse scattering into ray-tracing may require even more information of the materials, and in addition render tools even more computationally complex.

Recently, the so-called room electromagnetics (RE) theory has been introduced [4] that offers an alternative description of diffuse scattering in a room using only simple parameters like the room volume, area, and an absorption coefficient. This, surprisingly simple description may prove very useful when trying to model and simulate the propagation inside a room.

The concept of RE is new in the area of propagation in regular building rooms and so far relatively unexplored. The current work focus on issues which have not been addressed before, variations in RE parameters with frequency and polarization. In addition, the influence of the antenna's directional properties on RE parameters are investigated. The work presented is based on dual-band wideband multiple-input multiple-output (MIMO) radio channel measurements.

II. Room Electromagnetics

The theory of RE was developed in [4] with inspiration from acoustics (room acoustics) and is reviewed below in part. A single room is assumed to contain both the transmitter (Tx) and Rx antenna and only diffuse scattering is considered.

The power-delay profile (PDP) resulting from the diffuse power alone is given by

$$P(\tau) = \begin{cases} P_0 e^{-\tau/\tau_0}, & \tau \geq \tau_d \\ 0, & \tau < \tau_d \end{cases} \tag{1}$$

where power is normalized to the Tx power, τ_d is the delay of the first arriving signal, and the reverberation power (RP) is given by

$$P_0 = \frac{\lambda^2}{(4\pi)^2} \frac{c\Delta}{V} \eta_{\text{pol}} \tag{2}$$

where c is the speed of light, λ is the wavelength, Δ is the pulse width, the total volume of the room is V, and the ratio of power coupled from the Tx polarization to Rx polarization is given by η_{pol}. Note that P_0 is independent of the wall absorption.

The reverberation time (RT) is given by

$$\tau_0 = \frac{4V}{c\eta A} \tag{3}$$

where A is the total area of the energy absorbing walls, floor and ceiling, η is the ratio of the incident power absorbed by the walls, and V is again the total volume of the room. Note that both the RP in (2) and the RT in (3) are independent of the antenna directivity, due to the signals being received randomly from all directions.

III. MEASUREMENTS

The measured data were obtained using a MIMO channel sounder based on the correlation principle. Up to 16 Tx channels may be measured truly simultaneously, each branch with 1 W transmit power. On the Rx side eight channels are measured in parallel, and using switching each branch can be extended so that in total 64 Rx channels are measured. Additional information about the sounder is available in [5]. For the current work 4 Tx and 64 Rx channels were used and the full complex wideband 4×64 MIMO channel was measured in a time-triggered way at a rate of 60 Hz in 10 s. This ensures proper sampling of the channel which is changing due to external changes, such as movements by people, *etc.* Each measured impulse response (IR) is 2000 samples long with a sampling increment of 2.5 ns, but due to the room dimensions only a small part of the delay range is used.

The 64 Rx channels are split in two, so that one half was measured with a carrier frequency of 2.3 GHz and the other half used a carrier frequency of 5.8 GHz, with simultaneous measurements on both frequencies. In a post-measurement processing procedure the measurements are compensated for the sounder system response and the bandwidth is limited to about 100 MHz. The resulting resolution of about 15 ns is sufficient to allow estimation of the RT, as shown in the following.

The Tx antennas are four vertically polarized omnidirectional broadband antennas, fed with the combined signals for the 2.3 GHz and 5.8 GHz carriers.

A. Spherical Horn Antenna Array

On the Rx side a spherical array of horn antennas is used. The 16 dual-polarized, broadband horns are arranged to point in different directions to cover the most important parts of a sphere. Measuring with this array allows investigations of the directional properties of the signals received. Due to the wideband properties each horn antenna can be used at both 2.3 GHz and 5.8 GHz. The array is depicted in Fig. 1.

The coupling between the two polarizations of the horns is less than -20 dB at 2.3 GHz and less than -27 dB at 5.8 GHz The full-width half-maximum beamwidth is about 55° at 2.3 GHz and about 40° at 5.8 GHz. The main directions of the horn antennas are given in Table I. More details about the horn antennas and the array are available in [6].

B. Measurement Locations

Fig. 2 illustrates the seminar room in which the measurements took place. The room contains ten tables and associated chairs, and also has a few mostly empty bookshelves and cabinets. The west side of the room consists mainly of windows, while the floor and ceiling are made of concrete. A lowered ceiling of plasterboard is also present.

The array of four Tx antennas was located next to the east wall on a wooden pole, at a height of approximately 2.14 m to mimic the location of a typical wireless network access point. The array was linear, with element distance of 26 cm, and aligned with the wall.
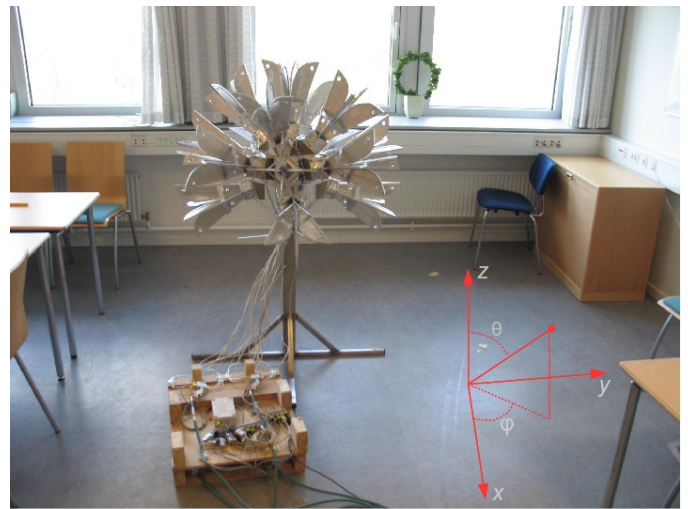

Fig. 1. The spherical array with 16 dual-polarized horn antennas. The coordinate system used to specify the horn directions is also sketched.
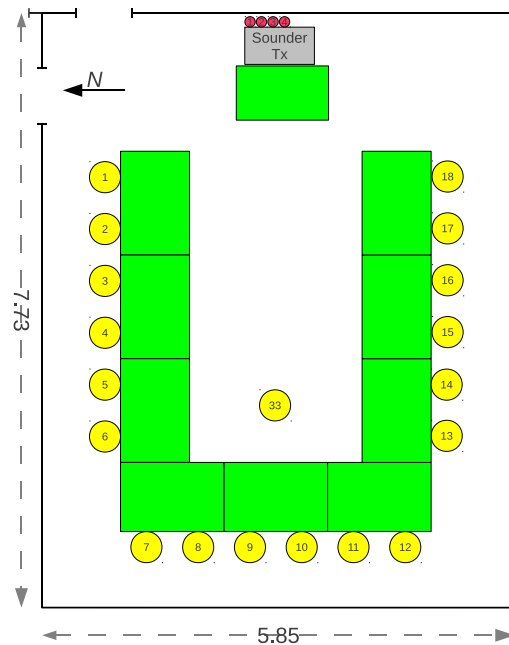

Fig. 2. Sketch of the seminar room with the measurement locations indicated.

Four of the locations labeled in Fig. 2 were used, R1, R7, R12, R18. For each of these main locations, four measurements were made with the spherical array placed at the corners of a 1 m by 1 m square centered at the main location, so that in total 16 measurements were made. Before the placement of the spherical array the nearby tables were moved to make room.

Note that the current work only treats one of the measurements made at each of the main locations; these are labelled R1.1, R7.1, R12.1, R18.1.

TABLE I

DIRECTIONS OF HORN ANTENNAS IN THE SPHERICAL ARRAY. THE ANGLES ARE GIVEN IN A COORDINATE SYSTEM WHERE THE θ ANGLE IS MEASURED FROM THE VERTICAL $z-axis$ AND THE ϕ ANGLE IS MEASURED FROM AN x-AXIS POINTING EAST. THE COORDINATE SYSTEM IS DEPICTED IN FIG. 1

Horn no.	1	2	3	4	5	6	7	8	9	10	11	12	13	14	15	16
θ [°]	110	110	110	110	75	75	75	75	75	75	75	40	40	40	40	0
ϕ [°]	0	90	180	270	9	63	118	172	226	281	335	18	108	198	288	–

IV. MEASUREMENT PROCESSING

Denoting by $h_i(p,q,m,n)$ a complex sample of the measured IR at time-index m, delay-index n, for the p-th Tx antenna, q-th Rx antenna, and measured at the i-th location in the room, the PDP is computed as

$$G_i(q,n) = \frac{1}{PM} \sum_{p=1}^{P} \sum_{m=1}^{M} |h_i(p,q,m,n)|^2 \qquad (4)$$

where the Rx antenna index represents any combination of direction, polarization, and band, *i.e.*, in total $16 \cdot 2 \cdot 2 = 64$ possibilities. In (4), $P = 4$ is the number of Tx, and $M = 600$ is the number of IR time samples. Thus, the PDP for each combination is obtained as the mean over both the four Tx antennas and all the time samples obtained at the same location.

With the purpose of investigating the data according to the RE theory, two regions of the PDP is defined:

'Header' This region is defined in the beginning of the PDP, possibly containing a line of sight (LOS) component. This region is defined as the first 2.5–25 ns of delay, corresponding to about 0.75–7.5 m, and chosen in correspondence with the delay resolution.

'Tail' This region is defined from the end of the header to the end of the delay. In practice the tail is defined in the delay region 27.5–193 ns, where the end point is chosen to result in power levels above the noise floor, determined by visual inspection of the PDP.

The tail region is where the diffuse scattering components are expected to be dominant. According to (1), the power received from diffuse scattering is exponentially decreasing and therefore the RT, τ_0, may be estimated from the slope of the tail region of the PDP in dB. The slope of the best linear fit to the PDP in the tail region is used, minimizing the squared error. In addition, RP, P_0 of (1), is estimated from the additive constant of the linear fit.

V. RESULTS

Fig. 3 shows some examples of the measured PDPs and the corresponding model curves fitting the tail region of the measured PDP. The curves shown are all for position R12.1, where the plots are for the four combinations of the two bands and two polarizations. For each plot four of the 16 horn antenna directions are shown, specifically directions approximately separated in azimuth by 90° and for $\theta = 75°$.

A first observation from Fig. 3 is that in many cases the linear decay of the model curves is a good fit to the measured data, but there are also deviations in some cases. The linear decay of the model curve is not expected to fit LOS components, and this is likely what is seen for $\phi = 9°$ in the plots for the θ-polarization. The first peak of these curves are around 10 ns. Approximately 55 ns later on the same curves, the next major peaks are observed. This delay difference corresponds to about 16.5 m of distance, which is comparable to two times the room dimension in the east-west direction. Hence, it is likely that these contributions are due to specular reflections on the walls to the east and west, thus explaining the major deviations from the model curve assuming diffuse scattering. Also note that similar peaks are found on the $\phi = 172°$ curves, *i.e.*, for the horn pointing approximately in the opposite direction. For the curves representing the approximate north and south directions, the peaks are much less distinctive.

It is interesting to note the $\phi = 9°$ curve for the ϕ-polarization, high band. The first peak of this curve occurs at about 20 ns, *i.e.*, later than for the first arriving signal of the θ-polarization. Since the Tx signal is mainly θ-polarized, the LOS component must be weak when receiving in the ϕ-polarization. This and the later arrival, indicates that the first peak seen in the ϕ-polarization is due to a specular reflection on one of the side walls, where coupling from the θ- to the ϕ-polarization takes place. In addition, the power level of the main peaks in the θ-polarization is higher than similar peaks in the ϕ-polarization, also supporting the notion that the latter are due to reflection.

Concerning the difference in power due to the carrier frequency, it is expected that the high band has lower power due to the antenna. Using (2), about 8 dB less power is expected in the high band, which is also approximately what is seen in the plots of the linear curves.

A. Statistics on reverberation time (RT)

Fig. 4 shows statistics of the RT, τ_0, for all combinations of the four locations R1.1, R7.1, R12.1, R18.1, the two bands and the two polarizations. For each combination statistics are computed from the RT values obtained for the 16 individual directions of the spherical array. Each combination is given on the x-axis, where the median is shown as the center (red) line, and the lower and upper limits of the (blue) box indicate the 25% and 75% percentile, respectively. The (red) dashed lines extend to the most extreme data points, except outliers, shown with (red) '+'. A data point is labelled as an outlier if the distance to the nearest 25% or 75% percentile is larger than 1.5 times the distance between the two percentiles. The
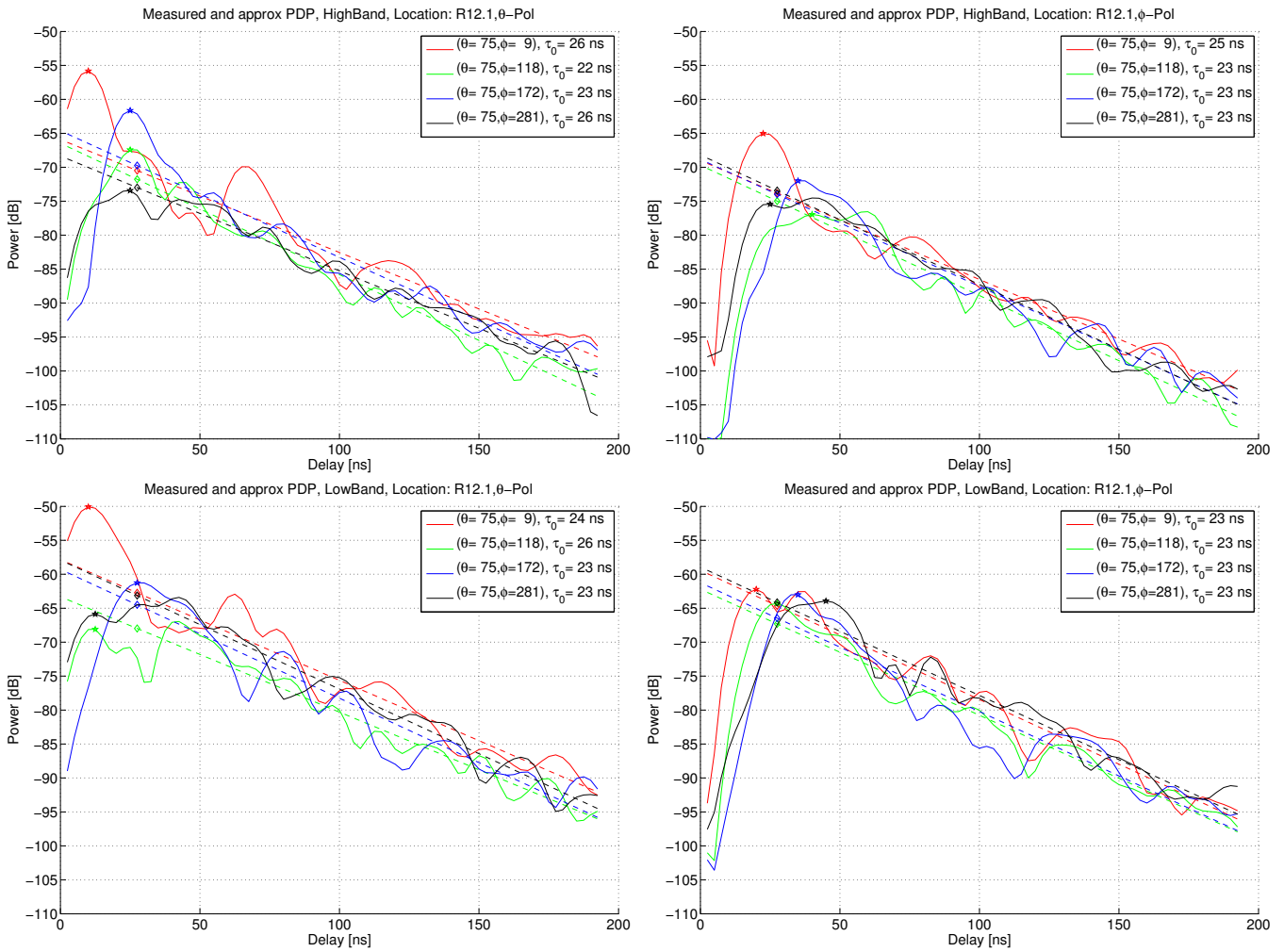
Fig. 3.   Measured PDP and linear approximation of tail region, shown for four ϕ-directions (azimuth) for the R12.1 location. Low band (bottom row), High band (top row), θ-polarization (left column), ϕ-polarization (right column).

notches in the blue boxes near the median values indicate the 95% confidence intervals of the medians.

Although the estimated RT values range from about 19 ns to 35 ns, including outliers, the statistics in the figure indicate that most values are within a fairly small range, with all median values in the range 22.1–24.6 ns.

For the high band, the median RT is always smaller for the ϕ-polarization than for the θ-polarization, of the order 1 ns, although the differences are small compared to the confidence intervals. For the low band, the differences in median RT are generally small.

In addition, there is a tendency that the RT for the low band is slightly smaller than for the high band, about 0.3 ns is mean. Again, the differences are small compared to the estimated confidence intervals and hardly significant.

Also the differences in the median values for the four locations are small.

B. Statistics on reverberation power (RP), P_0

Similar to Fig. 4, a boxplot of the estimated P_0 values is shown in Fig. 5. The most obvious observation to make is the clear difference in P_0 between the two bands. As mentioned above, it is expected that the received power in the high band is lower than on the low band, with a mean difference in the observed median values of about 9.5 dB. This is higher than the anticipated about 8 dB, from (2). A possible explanation is offsets in the median values due to specular components in the measurements.

There is a tendency on the high band that the medians for the θ-polarization is higher than for the ϕ-polarization, with differences of 0.2–1.3 dB. The differences are, however, small compared to the estimated confidence intervals.

A reverse tendency may be present on the low band, *i.e.*, that the ϕ-polarization has higher power than the θ-polarization. With the exception of the R7.1 location, the median differences are 1.2–1.7 dB. But again, these differences are small compared to the confidence intervals.
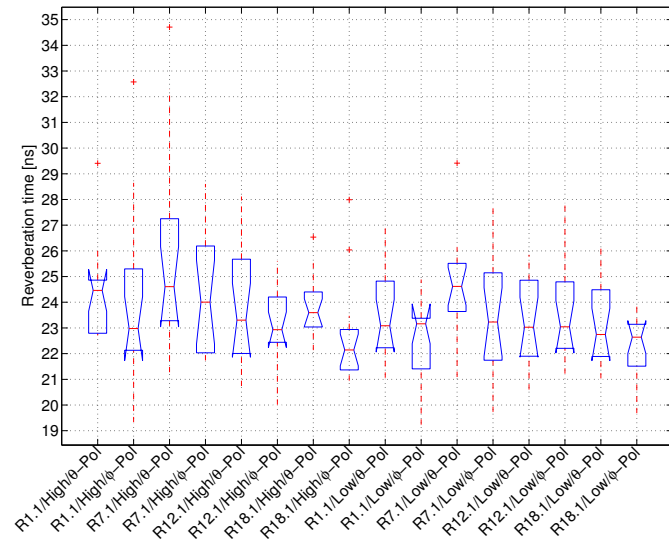
Fig. 4. Statistics of the reverberation time (RT), τ_0, for all combinations of location, polarization, and frequency band.
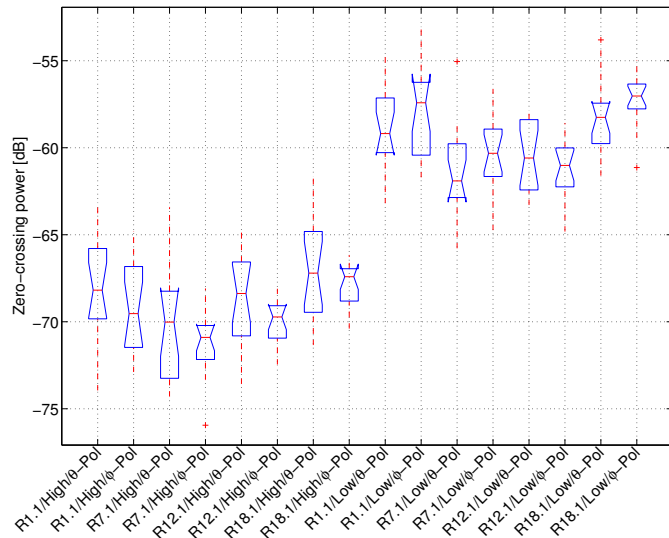

Fig. 5. Statistics of the RP, P_0, for all combinations of location, polarization, and frequency band.

ϕ-polarization than for the θ-polarization. However, although the differences seem clearly present they are too small to be statistically significant for the given sample size.

Also statistics on the RP, *i.e.*, the constant of the linear fit, was examined. The RP is expected from theory to be about 8 dB smaller on the high band than on the low band. A difference of medians of about 9.5 dB was found from the measurements. Small differences in the medians of up to about 1.7 dB were found due to the polarization, but again found to be small compared to the uncertainty.

REFERENCES

[1] F. Saez de Adana, O. Gutierrez Blanco, I. Gonzalez Diego, J. Perez Arriaga, and M. Catedra, "Propagation model based on ray tracing for the design of personal communication systems in indoor environments," *IEEE Transactions on Vehicular Technology*, vol. 49, no. 6, pp. 2105–2112, Nov. 2000.
[2] Y. Lostanlen and G. Gougeon, "Introduction of diffuse scattering to enhance ray-tracing methods for the analysis of deterministic indoor UWB radio channels (invited paper)," in *Electromagnetics in Advanced Applications, 2007. ICEAA 2007. International Conference on*, Sep. 2007, pp. 903–906.
[3] F. Mani and C. Oestges, "Evaluation of diffuse scattering contribution for delay spread and crosspolarization ratio prediction in an indoor scenario," in *Antennas and Propagation (EuCAP), 2010 Proceedings of the Fourth European Conference on*, Apr. 2010, pp. 1–4.
[4] J. B. Andersen, J. Ø. Nielsen, G. F. Pedersen, G. Bauch, and M. Herdin, "Room electromagnetics," *Antennas and Propagation Magazine, IEEE*, vol. 49, no. 2, pp. 27–33, Apr. 2007.
[5] J. Ø. Nielsen, J. B. Andersen, P. C. F. Eggers, G. F. Pedersen, K. Olesen, E. H. Sørensen, and H. Suda, "Measurements of indoor 16×32 wideband MIMO channels at 5.8 GHz," in *Proceedings of the 2004 International Symposium on Spread Spectrum Techniques and Applications (ISSSTA 2004)*, 2004, pp. 864–868.
[6] O. Franek and G. F. Pedersen, "Spherical horn array for wideband propagation measurements," *IEEE Transactions on Antennas and Propagation*, no. 99, May 2011.

VI. CONCLUSION

The room electromagnetics (RE) theory results in a linear decay (in dB) of the PDP, independent of the antenna, assuming purely diffuse scattering. This work is based on measurements utilizing horn antennas pointing in different directions, allowing an investigation of the antenna independence of the RE theory. Some deviations are found from the linear decay, most likely due to specular reflections in the room. In other directions where specular reflections are not likely the measurements agree well with the RE theory.

The median reverberation time (RT) were found to be in the range of about 22–25 ns. Within this range it is found that the RT tends to be slightly smaller for the low band than for the high band, and that the RT tends to be slightly smaller for the